Original Article

Elongated axial length and myopia-related fundus changes associated with the Arg130Cys mutation in the *LIM2* gene in four Chinese families with congenital cataracts

Xun Wang[1], Yanli Qin[2], Aierxiding Abudoukeremuahong[2], Meimei Dongye[1], Xulin Zhang[1], Dongni Wang[1], Jing Li[1], Zhuoling Lin[1], Yahan Yang[1], Lin Ding[2], Haotian Lin[1]

[1]State Key Laboratory of Ophthalmology, Zhongshan Ophthalmic Center, Sun Yat-sen University, Guangzhou, China; [2]Department of Ophthalmology, People's Hospital of Xinjiang Uygur Autonomous Region, Urumqi, China

Contributions: (I) Conception and design: H Lin, L Ding; (II) Administrative support: H Lin; (III) Provision of study materials or patients: H Lin, L Ding; (IV) Collection and assembly of data: X Wang, Y Qin, A Abudoukeremuahong, D Wang, M Dongye, X Zhang, J Li, Z Lin, Y Yang; (V) Data analysis and interpretation: X Wang, D Wang; (VI) Manuscript writing: All authors; (VII) Final approval of manuscript: All authors.

Correspondence to: Haotian Lin. Zhongshan Ophthalmic Center, Sun Yat-sen University, 54 Xian Lie South Road, Guangzhou 510060, China. Email: gddlht@aliyun.com; Lin Ding. Department of Ophthalmology, People's Hospital of Xinjiang Uygur Autonomous Region, 91 Tianchi Road, Urumqi 830001, China. Email: dinglin85600@163.com.

Background: Congenital cataract (CC) is a congenital abnormality characterized by lens opacity present at birth and is associated with highly heterogeneous clinical manifestations. Lens-specific integral membrane protein (*LIM2*) gene expression is localized to tight junctional domains of different lens fiber membranes. To date, only four mutations in *LIM2* have been reported to be associated with congenital or presenile cataracts. Due to the rarity of variants detected in the gene, there is limited progress in understanding the correlation between the genotype and phenotype of patients with mutations in *LIM2*.

Methods: A total of four Chinese families with CCs were recruited for this study, including three families inheriting in an autosomal dominant (AD) pattern and one sporadic case. Genomic DNA was extracted from the leukocytes of peripheral blood collected from all available patients. Whole-exome sequencing (WES) was performed on all probands and at least one of their parents. Bioinformatics analysis was performed to evaluate the pathogenicity of the candidate variants. Exon 4 of *LIM2* was amplified by polymerase chain reaction and directly sequenced. All patients underwent full ocular examinations. This was an observational study to explore the genotype-phenotype relationships in the four families with a common candidate variant.

Results: Various ocular phenotypes were detected in these families, mainly including CCs, elongated axial length, and myopia-related fundus changes. The *LIM2* gene mutation, p.Arg130Cys, was detected in all patients. This was further confirmed by Sanger sequencing. The proportion of probands with this mutation in our CCs database was 3.1% (4/130), which indicated that this mutation appears to be a frequent cause of cataracts in the Han Chinese population. This variation has been reported by other investigators before and was correlated with isolated cataracts.

Conclusions: This is the first study that reports various ocular phenotypes associated with the p.Arg130Cys mutation in the *LIM2* gene, which indicated the phenotypic heterogeneity of this gene. *LIM2* might not only function as an integral membrane protein in lens fiber cells but also be associated with the axial development of the eyeball. Functional studies of the *LIM2* gene are important and should receive more attention.

Keywords: Lens-specific integral membrane protein (*LIM2*); congenital cataracts (CCs); whole-exome sequencing (WES); phenotype-genotype correlation

Submitted May 27, 2020. Accepted for publication Nov 13, 2020.
doi: 10.21037/atm-20-4275
View this article at: http://dx.doi.org/10.21037/atm-20-4275

Introduction

Congenital cataract (CC) refers to a congenital anomaly that occurs from the clouding of the ocular lens at birth. The global prevalence of CC ranges from 2.2–13.6 per 10,000 children (1). The heredity of CC is highly heterogeneous (2). According to the Cat-Map database, there are more than 300 genes/loci associated with cataracts (http://cat-map.wustl.edu, last updated on March 30, 2020). To date, approximately 22 of these can be inherited in both autosomal dominant (AD) and autosomal recessive (AR) patterns, including *EPHA2* (1p36.13), *FOXE3* (1p32), *GJA8* (1q21.1), *FLNB* (3p14.3), *BFSP2* (3q21–q22), *PITX3* (10q25), *LRP5* (11q13.4), *CRYAB* (11q22.1–q23.2), *MIP* (12q13), *GJA3* (13q11–q12), *NR2E3* (15q22.32), *POLG* (15q25), *HSF4* (16q21), *CRYBA1* (17q11.2–q12), *GALK1* (17q24), *LIM2* (19q13.4), *BFSP1* (20p11.23–p12.1), *CRYAA* (21q22.3), *CRYBB3* (22q11.23), *CRYBB1* (22q12.1), and *CRYBA4* (22q12.1) (3-27). There is also a large variability in the phenotypes of patients with CC. Under most circumstances, the genotype heterozygosity of CC can lead to various manifestations. On the other hand, even in patients with the same mutation, their phenotypes can also be variable.

The *LIM2* gene encodes the second most abundant lens-specific integral membrane protein, also known as MP19 or MP20. It is a member of the PMP-22/EMP/MP20/claudin (Pfam00822) family of proteins, with roles in intercellular adhesion and protein trafficking (28). To date, four variants of *LIM2* have been reported to be associated with the CCs. Three variants (p.Gly78Asp, p.Phe105Val and p.Gly154Glu) are inherited in an autosomal recessive mode (23,29,30). The other mutation reported was p. Arg130Cys, which is inherited in an AD pattern (22). To date, all four mutations have been described as associated with congenital or presenile cataracts. The morphologies of cataracts can be cortical sutural, nuclear and pulverulent. In the present study, four Chinese families in our CCs database (130 unrelated families in total) with the same p.Arg130Cys mutation in the *LIM2* gene were detected. Other than CC, patients in these four families featured various ocular phenotypic manifestations, including elongated axial length, myopia-related fundus changes, congenital nystagmus, esotropia, and persistent fetal vasculature (PFV). All specific information of the patients in this report was deidentified. We present the following article in accordance with the STROBE reporting checklist (available at http://dx.doi.org/10.21037/atm-20-4275) as an observational study to explore the genotype-phenotype relationships in the four families with a common candidate variant.

Methods

Patients

Eleven patients in four Chinese families (*Figure 1A*) were recruited from the Home for Cataract Children of Zhongshan Ophthalmic Center between January 2020 and May 2020. The study was conducted in accordance with the Declaration of Helsinki (as revised in 2013). The study was approved by the Institutional Review Board of Zhongshan Ophthalmic Center (No. 2020KYPJ007), and informed consent was provided by all the patients or their guardians. All included participants were diagnosed with CC at an early stage. A full ophthalmic examination was performed, including a best-corrected visual acuity assessment, slit-lamp biomicroscopy, fundus photography, B-ultrasound scan, and retinoscopy with cycloplegia, and ocular biometry measurements were performed with an A-ultrasound scan or IOL Master. The axial length data of four eyes from three patients were not collected due to eye atrophy or because the patients were too young to cooperate with the examination.

Mutation screening

Genomic DNA was extracted from leukocytes obtained from peripheral blood samples, as previously described (31). The molecular basis of all probands in four families was identified with whole-exome sequencing (WES) technology. The Agilent liquid phase chip capture system was utilized for efficient enrichment of whole-exome region DNA. Database building and capture assay were performed by the Agilent Sure Select Human All Exon V6 Kit (Agilent Technologies Inc., CA, USA). WES was performed on the Illumina platform (Illumina Inc., CA, USA) following a quality inspection. The human reference genome assembly (NCBI build 37/hg19) was used to map sequence reads by CLC Genomics Workbench (version 6.5.2) software (CLC bio, Aarhus, Denmark). After alignment to the human reference genome (GRCh37/hg19), frequencies of variants were determined from the 1,000 Genomes database (http://grch37.ensembl.org/Homo_sapiens/Info/Index, Sep. 2015 data release), and the gnomAD databases (141,456 individuals; Oct. 2018 data release), removing minor allele frequency (MAF) values that were greater

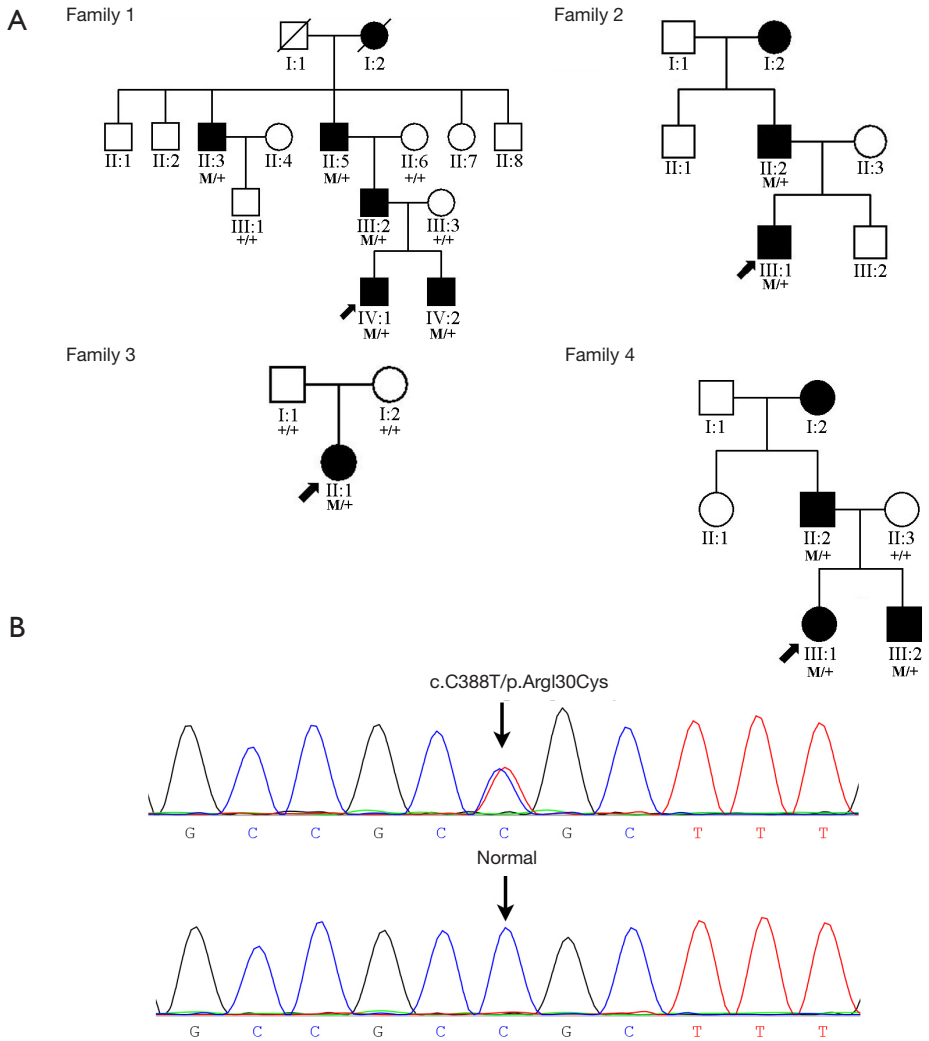

Figure 1 Pedigrees of the four families and sequencing results of the *LIM2* mutation. (A) Pedigrees and cosegregation analyses of four families with mutation p.Arg130Cys of *LIM2*. (B) Electropherogram of the involved sequence fragment of *LIM2* for the proband in family 1, the result of forward sequence is shown. The mutation is absent in the normal control III:3 in family 1.

than 0.0002. The frequency was based on the incidence of CCs (2.2/10,000). The PolyPhen-2 (32), SIFT (33) and MutationTaster (34) online tools were used to predict the pathogenicity of missense mutations on the coding regions. The pathogenicity of splice-site changes in the introns and synonymous variants in the exons were predicted using the Splice Site Prediction program with Neural Network (BDGP) (35). The candidate variants in 355 cataract-associated genes were selected for further validation by Sanger sequencing (http://cat-map.wustl.edu, last updated on March 30, 2020). In addition, the candidate variants in seven PFV-associated genes were also double-checked and validated (Table S1). Segregation analyses of mutations were performed for available family members.

Haplotype analysis

In addition to the proband in family 3, which was a sporadic case, the patients of the other three families all showed an AD inheritance pattern. Based on the WES results of the probands and their parents, the haplotypes of the three probands were analyzed to identify whether those families shared a common founder allele. Six single nucleotide polymorphisms (SNPs) within and flanking the *LIM2*

gene region were used for haplotype reconstruction, which spanned approximately 0.52 megabase (Mb) pairs. All SNPs met the variants' quality criteria of the WES results (36). The list of the SNPs and the haplotype analysis of the probands are shown in Table S2.

Statistical analysis

The association between elongated axial length and myopia-related fundus changes and the Arg130Cys mutation in the *LIM2* gene was determined using a two-tailed Fisher exact test. Analyses with P values <0.05 were considered significant. All statistical analyses were performed using the IBM SPSS Statistics 20 software (IBM Inc., New York, USA).

Results

Molecular findings

A heterozygous missense mutation c.C388T (p.Arg130Cys) in exon 4 of the *LIM2* gene was identified in all affected individuals. It was not detected in any unaffected family members nor in the 1,000 Genomes database or in the gnomAD databases. The mutation causes the arginine 130 codon (CGC) to change to a cysteine codon (TGC) in the second extracellular loop of the LIM2 protein. This mutation was previously reported to be associated with isolated CCs in a British family and a Czech family. The pedigrees, cosegregation analyses, and sequence maps of the four families with the mutation in the *LIM2* gene are shown in *Figure 1*.

Haplotype analysis and founder event identification

In the three families with an AD mode of inheritance, family 1 lived in Xinjiang Province for at least four generations in Northwest China. Families 2 and 4 came from two different cities in Jiangxi Province in Southeast China. The distance between the two provinces is more than 3,600 kilometers. The geographical positions of the four families are shown in Figure S1. Considering the close distance between the positions of families 2 and 4, the haplotypes of the probands in families 1, 2 and 4 were analyzed to identify whether they shared the same founder allele. In the analysis results, the haplotypes shared by the three probands was between rs12461542 and rs3794984, which spanned 0.41 Mb pairs. The region shared between family 1 and family 2 was 0.26 Mb pairs. The region shared between family 2 and family 4 spanned 0.19 Mb pairs, which was even shorter than the shared region between family 1 and family 2. Considering that the shared haplotype region of the three probands was quite limited, as well as taking into account the geographical distance between Xinjiang and Jiangxi Province, the three families may have had founder events that occurred independent from each other. The positions, intermarker distance and allele frequencies of the SNPs, and the haplotype analysis results of the probands in families 1, 2 and 4 are shown in Table S2.

Clinical data

Eleven patients (two female patients and nine male patients) and six normal members (four female members and two male members) from the four families were evaluated in this study. Bilateral CCs were diagnosed in all patients (11/11) at a median age of 7 months (ranging from 4 months to 10 years). The elongated axial length was found in 72.7% of the patients (8/11). The myopia-related fundus changes (including leopard-shaped fundus, patchy chorioretinal atrophy and optic disc change) were found in all of the eleven patients (11/11). None of the normal members in the four families carried the *LIM2* mutation nor had high myopia or myopia-related fundus changes. The prevalence of elongated axial length was statistically significantly higher in the patients' cohort (8/11, 72.7%) than in the normal member group (0/6, 0%, P=0.009). The prevalence of myopia-related fundus changes was statistically significantly higher in the patients' cohort (11/11, 100%) than in the normal member group (0/6, 0%, P=0.000). The summary of all ocular phenotypes of patients in the four families with the p.Arg130Cys mutation is shown in *Table 1*.

In family 1, all patients were diagnosed with bilateral cataracts before the age of 10 years. IV:1 was the proband. He was referred to the ophthalmic department for bilateral leukocoria at 4 months of age and was diagnosed with nuclear cataracts. His cataract phenotype was bilateral nuclear cataract surrounded by pulverulent cortical opacity. After undergoing cataract extraction and intraocular lens implantation surgery at 6 months, he was diagnosed with elongated axial length (23.17 mm OD, 23.07 mm OS), leopard-shaped fundus and optic disc tilt in both eyes at the age of 4 years and 5 months. IV:2 was the younger brother of IV:1. Differing from the nuclear cataract phenotype of IV:1, he had bilateral lamellar cataracts with a relatively transparent central area. He also had myopia-related fundus

Table 1 Clinical phenotypes of patients in the four families with the p.Arg130Cys mutation in *LIM2*

Individual ID	Inheritance patterns	Sex	Age at (year)		Lens morphology	Axis length at last-time examination (OD/OS mm)	Elongated axial length	Myopia related fundus changes			Others
			Presentation	On-set				Leopard-shaped fundus	Patchy chorioretinal atrophy	Optic disc changes (tilt/torsion/PPA)	
Family 1-II:3	AD	M	65 y	<10 y	Cataract OU	32.42/31.68	+	+	+	+	CN OU
Family 1-II:5		M	62 y	<10 y	Cataract OU	31.85/32.69	+	+	+	+	–
Family 1-III:2		M	35 y	5 y	Cataract OU	NA/23.86	–	+ (OS)	–	+ (OS)	Eyeball atrophy OD
Family 1-IV:1		M	4 y 5 m	4 m	Nuclear cataract surrounded by pulverulent cortical opacity OU	23.17/23.07	+	+	–	+	CN OU; IE OS
Family 1-IV:2		M	1 y 8 m	7 m	Lamellar cataract with relatively transparent central area, surround by pulverulent cortical opacity OU	NA/NA	NA	–	+	+	PFV OU, CN OU, IE OS
Family 2-proband	AD	M	3 y 9 m	6 m	Nuclear cataract surrounded by pulverulent cortical opacity OU	25.43/25.57	+	+	–	+	–
Family 2-II:2		M	34 y	Infancy	Cataract OU	27.88/NA	+ (OD)	+ (OD)	–	+ (OD)	Eyeball atrophy OS, CN OU
Family 3-proband	SC	F	4 y 8 m	2 y	Pulverulent cataract OD, posterior polar cataract OS	21.20/21.13	–	+	–	+	–
Family 4-proband	AD	F	5 y 1 m	7 m	Nuclear and posterior polar cataract OU	24.01/24.03	+	+	–	+	CN OU, AE OU
Family 4-II:2		M	29 y	10 y	Cataract OU	26.63/27.05	+	+	–	+	CN OU
Family 4-III:2		M	11 m	5 m	Irregular lamellar cataract surround by pulverulent cortical opacity OU	21.10/21.07	+	+	–	+	–

AD, autosomal dominant inheritance; SC, sporadic case; +, *LIM2* mutation exists; –, *LIM2* mutation does not exist; M, male; F, female; y, years; m, months; OD, the right eye; OS, the left eye; OU, both eyes; NA, not available; PPA, parapapillary atrophy; CN, congenital nystagmus; IE, intermittent esotropia; PFV, persistent fetal vasculature; AE, alternating esotropia.

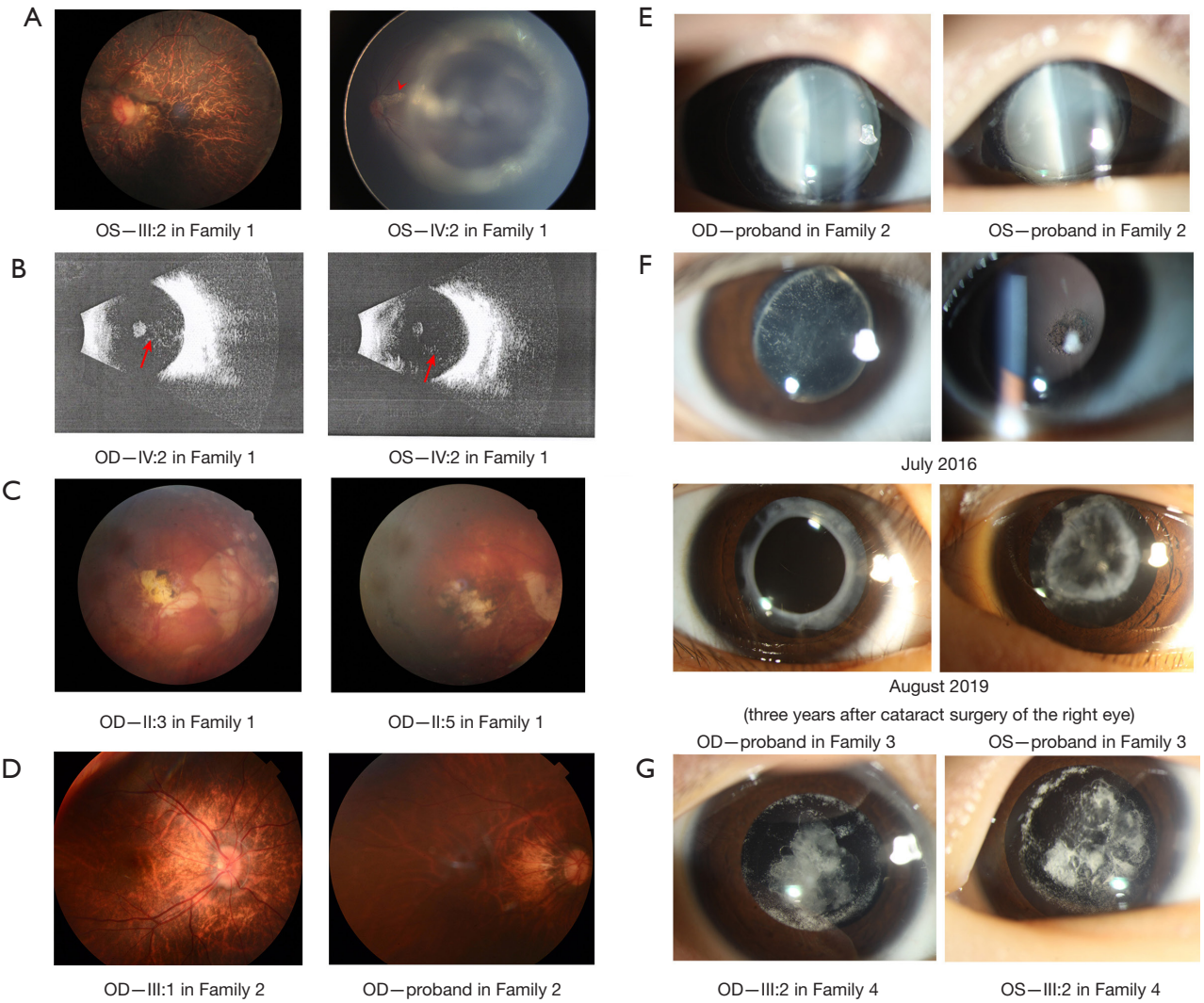

Figure 2 Ocular phenotypes of patients with CCs in the four families. (A) Left panel: fundus photo of the left eye of III:2 in family 1 showed severe leopard-pattern changes and an oval and tilt optic disc. Right panel: fundus photo of the left eye of IV:2 in family 1 showed PFV and posterior patchy chorioretinal atrophy (red arrow head). (B) B scan of IV:2 in family 1 showed fibrovascular stalk from the optic disc to the lens posterior capsule (red arrow). (C) Fundus photo of II:3 and II:5 in family 1, showed posterior patchy chorioretinal atrophy. (D) Fundus photo of II:2 and III:1 (the proband) in family 2, showed leopard-shaped fundus and optic disc changes. (E) The total cataract of III:1 in family 2. (F) The development of cataract type from posterior subcapsular cataract to perinuclear cataract of II:1 (the proband) in family 3. (G) The irregular lamellar cataracts surround by pulverulent cortical opacity of III:2 in family 4. CC, congenital cataract; PFV, persistent fetal vasculature.

changes, including patchy chorioretinal atrophy and optic disc tilt. In addition, there were plaques of remnant tissue sitting on the posterior face of the bilateral lens of IV:2. He was diagnosed with PFV at when he was 7 months old. The fundus photo and B-ultrasound scan of IV:2 are shown in *Figure 2A* (right panel) and *Figure 2B*. III:2 is the father of IV:1 and IV:2. He was diagnosed with bilateral cataracts and had cataract surgery when he was 5 years old. His right eyeball was atrophied. The axis length of his left eye was within normal limits (23.86 mm) when he was 35 years old. Nevertheless, he had severe leopard-pattern changes and an oval and tilt optic disc in the fundus of his left eye (*Figure 2A*, left panel). II:5 was the grandfather of IV:1, and II:3 was the elder brother of II:5. Both II:3 and II:5

had bilateral CCs, elongated axial length, posterior patchy chorioretinal atrophy and optic disc tilt (*Figure 2C*). The axial lengths of both eyes of II:3 and II:5 were longer than 31 mm. Other ocular phenotypes observed in family 1 include bilateral congenital nystagmus (II:3, IV:1, and IV:2) and intermittent esotropia of the left eye (IV:1 and IV:2).

Similar to family 1, all available patients in families 2, 3 and 4 had CCs, elongated axial length and/or myopia-related fundus changes. Family 2 and family 4 inherited in an AD mode, and the patient in family 3 was a sporadic case. The proband of family 2 (III:1) was a 4-year-old boy. His axis lengths were larger than 25 mm in both eyes before he was 4 years old. He had bilateral leopard-shaped fundus and optic disc tilt (*Figure 2D*, right panel). The phenotypes of his cataracts were nuclear opacities surrounded by white dots (*Figure 2E*). His father also had long eye axial lengths and myopic fundus (*Figure 2D*, left panel). The proband of family 3 was a sporadic female case with a bilateral asymmetric cataracts phenotype. She had a pulverulent cataract in the right eye and a posterior polar cataract in the left eye when she was 2 years old. Three years later, her left eye developed into a lamellar cataract with pulverulent dots in the cortex, which differed from the cataract phenotype in her right eye (*Figure 2F*). The proband of family 4 was diagnosed with bilateral nuclear and posterior polar cataracts and had cataract surgery at the age of 7 months. Her younger brother III:2 had irregular lamellar cataracts surround by pulverulent cortical opacity in both eyes (*Figure 2G*). All patients in family 4 had long axial length and related fundus changes. The axial length data was not collected in the right eye of III:2 or either eye of IV:2 from family 1 or in the left eye of II:2 from family 2, because the eyes of III:2 and II:2 atrophied at approximately 30 years of age and IV:2 was too young to cooperate for the A-ultrasound scan examination. The ocular phenotypes of families 1–4 are shown in *Figure 2*.

Discussion

In this study, we report four Chinese families with the same c.C388T (p.Arg130Cys) mutation in the *LIM2* gene among 130 unrelated CCs families and sporadic cases. Haplotype analysis showed that the four families may have had founder events independent from each other. The proportion of probands with this mutation in our CCs database was 3.1% (4/130). This mutation appears to be a frequent cause of cataracts in the Han Chinese population. New phenotypes detected in the four families included elongated axial length, myopia-related fundus anomalies (leopard-shaped fundus, patchy chorioretinal atrophy and optic disc change), congenital nystagmus, esotropia, PFV and eyeball atrophy. Of them, elongated axial length and/or myopia-related fundus anomalies were consistently present in all available patients. The occurrence of other phenotypes, including congenital nystagmus, esotropia, and eyeball atrophy in multiple members of two or three of the families might be complications associated with the elongated axial length. The ocular phenotypes presented in this study were more than an isolated structural abnormality of the lens described in previous literature for patients with mutations in the *LIM2* gene (22,23,29,30).

The *LIM2* gene is a 20-kDa membrane protein with four intramembrane domains (37). It is expressed mainly in the cortical region of the lens and is localized to tight junctional domains of different lens fiber membranes (38-40). It may play an essential role in both lens development and cataractogenesis. The first mutation of *LIM2* associated with cataract (p.Gly15Val) was identified within the first coding exon in the cataractous To3 (total opacity of lens #3) mouse model (41). Phenotypic heterogeneity existed in both homozygous and heterozygous mice: heterozygous To3 mice had isolated dense opacities of the lens, while homozygous ones had dense cataracts and abnormally small eyes. Another mouse model with the *LIM2* p.Cys51Arg mutation displayed similar phenotypes as the To3 mice: the heterozygous mice were only affected with smaller lenses and eyes, and the homozygotes had nuclear cataracts and further reduced lens and eye sizes (42). Both mouse models above indicate a semidominant mode of inheritance. Different from the mouse models with missense mutations, a gene-trap mouse model that was functionally null for *LIM2* showed an autosomal recessive pattern of inheritance. Only homozygous gene-trap mice ($LIM2^{Gt/Gt}$) were observed with central pulverulent cataracts (43,44). In the aspect of histological analysis, all affected mouse models showed disorganized lens fiber layers in the lens cortex, which might reduce lens stability and lead to refractive defects (41-43). A summary of all reported *LIM2* mutations associated with cataracts in mouse models is shown in *Table 2*.

The *LIM2* gene mutation detected in this study, p.Arg130Cys, was the only AD mutation of the *LIM2* gene associated with CCs in humans. It corresponds to an arginine for cysteine substitution at residue 130, which is in the second extracellular loop of *LIM2* (45). Unlike the three autosomal recessive mutations associated with isolated cataracts, elongated axial length and/or myopia-related

Table 2 Summary of all reported *LIM2* mutations associated with cataracts

Species	Mutation	Inherited pattern	Genotype	Onset pattern	Phenotype	Histology	Mutation position in protein	Report
Mice	p.Gly15Val	Semidominant	Hom	Congenital	Total opacity of the lens, microphthalmia	Lens vacuolization and ruptured lens capsules	The first transmembrane domain	Steele *et al.* 1997
			Het	Congenital	Total opacity of the lens			
Mice	p.Cys51Arg	Semidominant	Hom	Congenital	Nuclear cataract, decreased sizes of eye axis and lens	Reduced stability and less organized fiber layer arrangement	The first extracellular loop	Puk *et al.* 2011
			Het	Congenital	Decreased sizes of eye axis and lens	No alterations found		
Mice	*LIM2* gene trap	AR	Hom		Central pulverulent cataract	Lacked the undulating morphology of wild-type fiber cells and decreased expression levels of the gap junction protein connexin 46 and absence of cell fusions in the lens core	Knock out of the entire gene	Shiels *et al.* 2007, Shi *et al.* 2011
Human	p.Phe105Val	AR	Hom	Presenile	Pulverulent cortical cataract	NA	The third transmembrane domain	Pras *et al.* 2002
Human	p.Gly154Glu	AR	Hom	Congenital	Total cataract, amblyopia and nystagmus	NA	The fourth transmembrane domain	Ponnam *et al.* 2008
Human	p.Gly78Asp	AR	Hom	Congenital	Nuclear cataract	NA	The first extracellular loop	Irum *et al.* 2016
Human	p.Arg130Cys	AD	Het	Congenital	Pulverulent and nuclear cataract, posterior polar cataract*, lamellar cataract*, elongated axial length*, myopia related fundus changes*	NA	The second extracellular loop	Berry *et al.* 2020, the present study

*, new phenotypes observed in this study. AR, autosomal recessive inheritance; AD, autosomal dominant inheritance; hom, homozygous; het, heterozygous; NA, not available.

fundus changes were present in all affected members with the p.Arg130Cys mutation in this study. Thus, myopia is more likely to be due to the axial nature rather than being secondary to cataracts. Two of the 11 patients in this study developed unilateral eyeball atrophy at approximately 30 years of age. This indicated that patients with this mutation may have a higher risk of retinal detachment. It was necessary for them to receive regular fundus examinations to avoid severe complications associated with high myopia. A summary of all reported *LIM2* mutations associated with cataracts in human beings and cataract phenotypes of the patients is shown in *Table 2*.

Our research indicated that the *LIM2* gene could be a candidate gene for early-onset myopia, especially in patients with CCs. There were some limitations to this study. One limitation was that the number of patients recruited in this study was limited. Further exploration of this mutation's genotype-phenotype relationship could be carried out in a larger cohort or in other populations. The other limitation was the lack of basic experiments on the pathological mechanism of the relationship of cataracts and myopia with this mutation. The underlying molecular mechanism between this mutation in the *LIM2* gene and myopia remains unknown. The function of the *LIM2* gene might be related with the increased remodeling and creep rate of scleral matrix during the embryonic and postnatal period (46). It is necessary to further study the relationship between the p.Arg130Cys mutation in the *LIM2* gene and myopia in cell or animal models. It might offer more information for identifying key gene signaling pathways and exploring specific molecular mechanisms of myopia.

Conclusions

The phenotypes of patients with CCs have a high heterogeneity. In this study, we first reported new phenotypes, including elongated axial length and myopia-related fundus changes in four Chinese families with a p.Arg130Cys mutation in the *LIM2* gene. This study could extend the understanding of the function of the *LIM2* gene and give insight into the relationship between lens fiber cell differentiation and the axial development of the eyeball. The importance of the *LIM2* gene in mutation screening of Chinese CC patients and a further study of its function are needed.

Acknowledgments

We would like to sincerely thank the patients and their families for their kind participation in the study and the China Standard Map Service Website (http://bzdt.ch.mnr.gov.cn/) to provide a map of China in Figure S1. We are also very grateful to Mr. Bryan Spencer and professional English editors in *American Journal Experts* Editing Service (https://www.aje.com/) for their help in language editing.

Funding: This work was supported by the National Natural Science Foundation of China (81822010, 81770967); and the Science and Technology Planning Projects of Guangdong Province (2019B030316012).

Footnote

Reporting Checklist: The authors have completed the STROBE reporting checklist. Available at http://dx.doi.org/10.21037/atm-20-4275

Data Sharing Statement: Available at http://dx.doi.org/10.21037/atm-20-4275

Peer Review File: Available at http://dx.doi.org/10.21037/atm-20-4275

Conflicts of Interest: All authors have completed the ICMJE uniform disclosure form (available at http://dx.doi.org/10.21037/atm-20-4275). Dr. HL reports grants from National Natural Science Foundation of China (81822010), grants from National Natural Science Foundation of China (81770967), grants from Science and Technology Planning Projects of Guangdong Province (2019B030316012), during the conduct of the study. The other authors have no conflicts of interest to declare.

Ethical Statement: The authors are accountable for all aspects of the work in ensuring that questions related to the accuracy or integrity of any part of the work are appropriately investigated and resolved. The study was conducted in accordance with the Declaration of Helsinki (as revised in 2013). The study was approved by the Institutional Review Board of Zhongshan Ophthalmic Center (No. 2020KYPJ007) and informed consent was taken from all the patients or their guardians.

References

1. Wu X, Long E, Lin H, et al. Prevalence and epidemiological characteristics of congenital cataract: a systematic review and meta-analysis. Sci Rep 2016;6:28564.
2. Pichi F, Lembo A, Serafino M, et al. Genetics of congenital cataract. Dev Ophthalmol 2016;57:1-14.
3. Musleh M, Hall G, Lloyd IC, et al. Diagnosing the cause of bilateral paediatric cataracts: comparison of standard testing with a next-generation sequencing approach. Eye (Lond) 2016;30:1175-81.
4. Patel N, Anand D, Monies D, et al. Novel phenotypes and loci identified through clinical genomics approaches to pediatric cataract. Hum Genet 2017;136:205-25.
5. Iseri SU, Osborne RJ, Farrall M, et al. Seeing clearly: the dominant and recessive nature of FOXE3 in eye developmental anomalies. Hum Mutat 2009;30:1378-86.
6. Zhang L, Liang Y, Zhou Y, et al. A missense mutation in GJA8 encoding connexin 50 in a Chinese pedigree with autosomal dominant congenital cataract. Tohoku J Exp Med 2018;244:105-11.
7. Ma AS, Grigg JR, Ho G, et al. Sporadic and familial congenital cataracts: mutational spectrum and new diagnoses using next-generation sequencing. Hum Mutat 2016;37:371-84.
8. Liu Q, Wang KJ, Zhu SQ. A novel p.G112E mutation in BFSP2 associated with autosomal dominant pulverulent cataract with sutural opacities. Curr Eye Res 2014;39:1013-9.
9. Aldahmesh MA, Khan AO, Mohamed J, et al. Novel recessive BFSP2 and PITX3 mutations: insights into mutational mechanisms from consanguineous populations. Genet Med 2011;13:978-81.
10. Semina EV, Ferrell RE, Mintz-Hittner HA, et al. A novel homeobox gene PITX3 is mutated in families with autosomal-dominant cataracts and ASMD. Nat Genet 1998;19:167-70.
11. Ye X, Zhang G, Dong N, et al. Human pituitary homeobox-3 gene in congenital cataract in a Chinese family. Int J Clin Exp Med 2015;8:22435-9.
12. Jiao X, Khan SY, Irum B, et al. Missense mutations in CRYAB are liable for recessive congenital cataracts. PLoS One 2015;10:e0137973.
13. Xiao X, Li W, Wang P, et al. Cerulean cataract mapped to 12q13 and associated with a novel initiation codon mutation in MIP. Mol Vis 2011;17:2049-55.
14. Chen J, Wang Q, Cabrera PE, et al. Molecular genetic analysis of Pakistani families with autosomal recessive congenital cataracts by homozygosity screening. Invest Ophthalmol Vis Sci 2017;58:2207-17.
15. Yao K, Wang W, Zhu Y, et al. A novel GJA3 mutation associated with congenital nuclear pulverulent and posterior polar cataract in a Chinese family. Hum Mutat 2011;32:1367-70.
16. Micheal S, Niewold ITG, Siddiqui SN, et al. Delineation of novel autosomal recessive mutation in GJA3 and autosomal dominant mutations in GJA8 in Pakistani congenital cataract families. Genes (Basel) 2018;9:112.
17. Bu L, Jin Y, Shi Y, et al. Mutant DNA-binding domain of HSF4 is associated with autosomal dominant lamellar and Marner cataract. Nat Genet 2002;31:276-8.
18. Qi Y, Jia H, Huang S, et al. A deletion mutation in the betaA1/A3 crystallin gene (CRYBA1/A3) is associated with autosomal dominant congenital nuclear cataract in a Chinese family. Hum Genet 2004;114:192-7.
19. Khan AO, Aldahmesh MA, Alkuraya FS. Phenotypes of recessive pediatric cataract in a cohort of children with identified homozygous gene mutations (An American Ophthalmological Society Thesis). Trans Am Ophthalmol Soc 2015;113:T7.
20. Singh R, Ram J, Kaur G, et al. Galactokinase deficiency induced cataracts in Indian infants: identification of 4 novel mutations in GALK gene. Curr Eye Res 2012;37:949-54.
21. Kolosha V, Anoia E, de Cespedes C, et al. Novel mutations in 13 probands with galactokinase deficiency. Hum Mutat 2000;15:447-53.
22. Berry V, Pontikos N, Dudakova L, et al. A novel missense mutation in LIM2 causing isolated autosomal dominant congenital cataract. Ophthalmic Genet 2020;41:131-4.
23. Pras E, Levy-Nissenbaum E, Bakhan T, et al. A missense mutation in the LIM2 gene is associated with autosomal recessive presenile cataract in an inbred Iraqi Jewish family. Am J Hum Genet 2002;70:1363-7.
24. Li S, Zhang J, Cao Y, et al. Novel mutations identified in Chinese families with autosomal dominant congenital cataracts by targeted next-generation sequencing. BMC Med Genet 2019;20:196.
25. Hansen L, Yao W, Eiberg H, et al. Genetic heterogeneity in microcornea-cataract: five novel mutations in CRYAA, CRYGD, and GJA8. Invest Ophthalmol Vis Sci 2007;48:3937-44.
26. Riazuddin SA, Yasmeen A, Yao W, et al. Mutations in

betaB3-crystallin associated with autosomal recessive cataract in two Pakistani families. Invest Ophthalmol Vis Sci 2005;46:2100-6.
27. Jin A, Zhang Y, Xiao D, et al. A novel mutation p.S93R in CRYBB1 associated with dominant congenital cataract and microphthalmia. Curr Eye Res 2020;45:483-9.
28. Maher GJ, Black GC, Manson FD. Focus on molecules: lens intrinsic membrane protein (LIM2/MP20). Exp Eye Res 2012;103:115-6.
29. Ponnam SP, Ramesha K, Tejwani S, et al. A missense mutation in LIM2 causes autosomal recessive congenital cataract. Mol Vis 2008;14:1204-8.
30. Irum B, Khan SY, Ali M, et al. Mutation in LIM2 is responsible for autosomal recessive congenital cataracts. PLoS One 2016;11:e0162620.
31. Li L, Xiao X, Li S, et al. Detection of variants in 15 genes in 87 unrelated Chinese patients with Leber congenital amaurosis. PLoS One 2011;6:e19458.
32. Adzhubei IA, Schmidt S, Peshkin L, et al. A method and server for predicting damaging missense mutations. Nat Methods 2010;7:248-9.
33. Flanagan SE, Patch AM, Ellard S. Using SIFT and PolyPhen to predict loss-of-function and gain-of-function mutations. Genet Test Mol Biomarkers 2010;14:533-7.
34. Schwarz JM, Cooper DN, Schuelke M, et al. MutationTaster2: mutation prediction for the deep-sequencing age. Nat Methods 2014;11:361-2.
35. Houdayer C, Dehainault C, Mattler C, et al. Evaluation of in silico splice tools for decision-making in molecular diagnosis. Hum Mutat 2008;29:975-82.
36. Gilissen C, Hoischen A, Brunner HG, et al. Disease gene identification strategies for exome sequencing. Eur J Hum Genet 2012;20:490-7.
37. Arneson ML, Louis CF. Structural arrangement of lens fiber cell plasma membrane protein MP20. Exp Eye Res 1998;66:495-509.
38. Louis CF, Hur KC, Galvan AC, et al. Identification of an 18,000-dalton protein in mammalian lens fiber cell membranes. J Biol Chem 1989;264:19967-73.
39. Tenbroek E, Arneson M, Jarvis L, et al. The distribution of the fiber cell intrinsic membrane proteins MP20 and connexin46 in the bovine lens. J Cell Sci 1992;103:245-57.
40. TenBroek EM, Johnson R, Louis CF. Cell-to-cell communication in a differentiating ovine lens culture system. Invest Ophthalmol Vis Sci 1994;35:215-28.
41. Steele EC Jr, Kerscher S, Lyon MF, et al. Identification of a mutation in the MP19 gene, Lim2, in the cataractous mouse mutant To3. Mol Vis 1997;3:5.
42. Puk O, Ahmad N, Wagner S, et al. Microphakia and congenital cataract formation in a novel Lim2(C51R) mutant mouse. Mol Vis 2011;17:1164-71.
43. Shiels A, King JM, Mackay DS, et al. Refractive defects and cataracts in mice lacking lens intrinsic membrane protein-2. Invest Ophthalmol Vis Sci 2007;48:500-8.
44. Shi Y, De Maria AB, Wang H, et al. Further analysis of the lens phenotype in Lim2-deficient mice. Invest Ophthalmol Vis Sci 2011;52:7332-9.
45. Gonen T, Grey AC, Jacobs MD, et al. MP20, the second most abundant lens membrane protein and member of the tetraspanin superfamily, joins the list of ligands of galectin-3. BMC Cell Biol 2001;2:17.
46. Metlapally R, Wildsoet CF. Scleral mechanisms underlying ocular growth and myopia. Prog Mol Biol Transl Sci 2015;134:241-8.

Cite this article as: Wang X, Qin Y, Abudoukeremuahong A, Dongye M, Zhang X, Wang D, Li J, Lin Z, Yang Y, Ding L, Lin H. Elongated axial length and myopia-related fundus changes associated with the Arg130Cys mutation in the *LIM2* gene in four Chinese families with congenital cataracts. Ann Transl Med 2021;9(3):235. doi: 10.21037/atm-20-4275

Supplementary

Table S1 Genomic information of the seven PFV associated genes

Gene	Cytogenetic locus	gDNA	mRNA	Protein
NFKB1	4q24	NC_000004.11	NM_003998	NP_003989
VEGFA	6p21.1	NC_000006.11	NM_001025366	NP_001020537
EDN1	6p24.1	NC_000006.11	NM_001955	NP_001946
CDKN2A	9p21.3	NC_000009.11	NM_000077	NP_000068
ATOH7	10q21.3	NC_000010.10	NM_145178	NP_660161
TGFB1	19q13.2	NC_000019.9	NM_000660	NP_000651
NDP	Xp11.3	NC_000023.10	NM_000266	NP_000257

The human genome information was based on NCBI build 37/hg19. PFV, persistent fetal vasculature.

Table S2 The list of the SNPs and the haplotype analysis of the probands in family 1, 2 and 4

#Chromsome	Position	Intermarker distance (bp)	SNP ID	Haplotype of the mutant *LIM2* allele		
				F1-proband	F2-proband	F4-proband
19	51,608,074	–	rs2691249	C	C	A
19	51,689,700	81,626	rs12461542	T	C*	C*
19	51,837,332	147,632	rs10418551	G*	G*	G*
19	51,883,831	46,499	Mutation	A*	A*	A*
19	52,032,964	149,133	rs3976745	G*	G*	C
19	52,095,980	63,016	rs3794984	T*	T*	G
19	52,130,337	34,357	rs8105105	C	T	T
Distance of both ends of the shared haplotypes (bp)				258,648	406,280	194,131

* in haplotypes were the haplotypes shared between the three families. The human genome information of SNPs was based on UCSC NCBI build 37/hg19. SNP, single nucleotide polymorphism.

http://dx.doi.org/10.21037/atm-20-4275

Figure S1 The geographical positions of families 1, 2, 3 and 4 are shown in the map of China. The position of family 1 was in Urumqi, Xinjiang province. The position of family 2 was in Ji'an, Jiangxi Province. The position of family 3 was in Changning, Hunan province. The position of family 4 was in Ganzhou, Jiangxi province. The geographical distance between family 1 and families 2&4 is more than 3,600 kilometers. The geographical distance between family 3 and families 2&4 is around 400 kilometers. The geographical distance between family 2 and family 4 is around 200 kilometers. The map of China was download from the China Standard Map Service Website (http://bzdt.ch.mnr.gov.cn/) with the map approval number GS(2019)1696.

http://dx.doi.org/10.21037/atm-20-4275